

Application of electric field ionization method to detect the high-lying Rydberg states of Eu I

Jun Xie (谢 军), Changjian Dai (戴长建)*, and Ming Li (李 鸣)

¹Key Laboratory of Display Materials and Photoelectric Devices, Ministry of Education, Tianjin 300384, China

²School of Science, Tianjin University of Technology, Tianjin 300384, China

*Corresponding author: daicj@126.com

Received September 30, 2010; accepted January 3, 2011; posted online April 22, 2011

The $4f^7 6s(^9S)np\ ^8P_J$ ($J = 5/2, 7/2, 9/2$) Rydberg series converging to the first ionization limit $4f^7 6s\ ^9S_4$ of the Eu atom using the three-step laser excitation and electric-field-ionization (EFI) method are studied. First, the Eu atom is excited from the $4f^7 6s^2\ ^8S_{7/2}^o$ ground state to the $4f^7 6s7s\ ^8S_{7/2}^o$ state through the $4f^7 6s6p\ ^{10}P_{9/2}$ state by the first two dye lasers. Next, it is populated to many higher- n members of the $4f^7 6s(^9S)np\ ^8P_J$ Rydberg series by the third dye laser whose wavelength is scanned within a certain range. Finally, the atom in these higher- n states is ionized by the external pulsed electric field. With the field strength up to 2 kV/cm, we can detect the atom in $4f^7 6s(^9S)np\ ^8P_J$ states with $n \geq 40$. With the given laser line width, the level energies of Rydberg states with n as high as 72 can be determined. We not only confirm the previous data on the $4f^7 6s(^9S)np\ ^8P_J$ Rydberg series, but also extend the n -value assignment significantly by detecting more states.

OCIS codes: 020.0020, 020.5780, 300.0300, 300.6210.

doi: 10.3788/COL201109.050201.

Rydberg states of alkaline-earth atoms have been studied extensively^[1–3] due to their peculiar properties. Recently, Rydberg states of rare-earth atoms have also attracted much attention^[4–8]. Although there have been several studies on odd-parity Rydberg states of the Eu atom with multi-step resonance ionization spectroscopy^[5–8], the even-parity Rydberg series converging to the first ionization limit $4f^7 6s\ ^9S_4$ has only been investigated with traditional absorption spectroscopy^[9]. The higher members of the even-parity Rydberg series in particular have not been reported.

In this letter, we make the first attempt to study the Rydberg states of the Eu atom with the electric-field-ionization (EFI) method, which is well known to be a highly effective method for detecting higher members of Rydberg states. Although the EFI method has been very successfully utilized in studies of Rydberg states for simpler atoms with high selectivity and sensitivity^[10–12], it has never been applied to the Rydberg states of the Eu atom. With the EFI method, fruitful results on the $4f^7 6s(^9S)np\ ^8P_J$ ($J = 5/2, 7/2, 9/2$) Rydberg states have been obtained.

The experimental setup used in the present investigation is shown schematically in Fig. 1. It consists mainly of three parts: an atomic beam preparation system, a laser system, and a data acquisition system. The atomic beam preparation system, which is placed inside a vacuum chamber with a typical pressure of about 10^{-4} Pa, comprises an atomic oven, a heating facility, and a beam collimator. The atomic oven is heated resistively using a direct current (DC) power supply to a temperature of 760 K, which is monitored by a controller with a Platinum-Rhodium thermocouple attached to the oven. The laser system comprises three dye lasers pumped by the same Nd: YAG laser running at 20 Hz, which has a line-width of about 0.1 cm^{-1} and a pulse width of 6–8 ns. The data acquisition system includes a micro-

channel plate (MCP) detector, a digital pulse generator, and an integrated Boxcar connected with a computer.

The pulses of the second and third lasers are delayed properly to allow the three laser pulses to be sequential in time. To avoid Doppler broadening, the atomic beam is collimated and directed to a region between two electric field plates 1 cm apart and is crossed perpendicularly by the three laser beams. The three laser beams enter the vacuum chamber collinearly. To excite the Eu atom from the $4f^7 6s^2\ ^8S_{7/2}^o$ ground state to the $4f^7 6s7s\ ^8S_{7/2}^o$ state through the $4f^7 6s6p\ ^{10}P_{9/2}$ intermediate state, the wavelengths of the first two lasers, λ_1 and λ_2 , are fixed at 686.64 and 668.70 nm, respectively. Meanwhile, the wavelength of the third laser λ_3 is scanned within a certain range so that many Rydberg states can be populated, where the Eu atom is detected by the EFI. The three-step excitation scheme for producing the Rydberg atom can be shown as

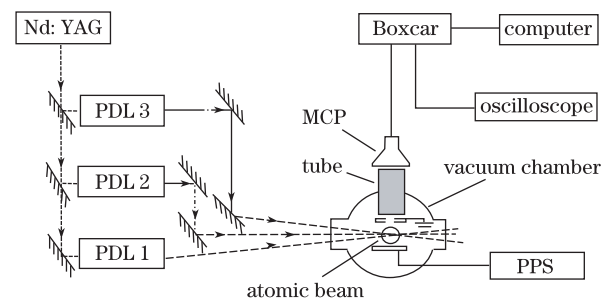


Fig. 1. Schematic diagram of the experimental apparatus, which consists of three parts: a laser system, an atomic beam preparation system, and a data acquisition system. The atomic beam is produced by an atomic oven in the vacuum chamber. The ion signal detected by a MCP is averaged by a Boxcar whose output is stored in a computer for further analysis. PDL: pulsed dye laser; PPS: pulsed power supply.

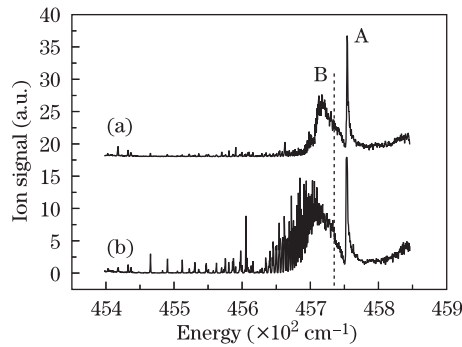
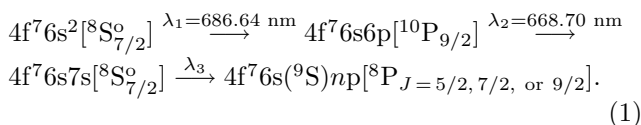


Fig. 2. Spectra of the Eu atom obtained from two different detection methods. (a) From photoionization; (b) from EFI. The broken line delineates the position of the first ionization limit.



To avoid the Stark effect, a pulsed electric field with high voltage is applied to the plates about $0.5 \mu\text{s}$ after the laser pulses. Ions from the EFI are sent to the data acquisition system described above for further analyses. To ionize a Rydberg state with an effective principal quantum number n^* , the applied electric field strength F should be greater than its EFI threshold, that is,

$$F \geq \frac{1}{16n^{*4}} \quad (\text{in atomic units}), \quad (2)$$

where n^* can be obtained from the Rydberg relation:

$$n^* = \sqrt{\frac{R}{T_0 - E}}, \quad (3)$$

where $R = 109,736.918 \text{ cm}^{-1}$ is the mass-corrected Rydberg constant for the Eu atom; $T_0 = 45,734.92 \text{ cm}^{-1}$ is the ionization limit of the Eu atom; E is the level energy obtained from experiment; an atomic unit of F is equal to $5.142 \times 10^9 \text{ V/cm}$.

To reduce possible errors in the experimental data, some steps have to be taken: (1) measure each spectrum several times and find the average to reduce random errors; (2) record the spectrum of an Fabry-Perot (F-P) etalon whose free spectral range is 2.4069 cm^{-1} to correct nonlinearity in the wavelength of the scanning dye laser; (3) calibrate the laser wavelength with the reference lines of a hollow cathode lamp; (4) shield the vacuum chamber from the external field with the μ metal; (e) set the time delay of the electric field pulse sufficiently to avoid any accidental Stark effect. Through the above steps, typical experimental uncertainties are estimated to be less than $\pm 0.1 \text{ cm}^{-1}$.

To demonstrate differences between the two detection methods, the spectra obtained from photoionization and the EFI are shown in Figs. 2(a) and (b), respectively. For the spectrum in Fig. 2(a), the Rydberg atom is ionized by absorbing another λ_3 photon, whereas for the spectrum in Fig. 2(b), it is obtained by applying a pulsed electric field of 2 kV/cm . For the states in the same energy region, the intensity of the third laser should be set to a higher level for photoionization. In comparison, only a lower level is necessary for the EFI process, in which

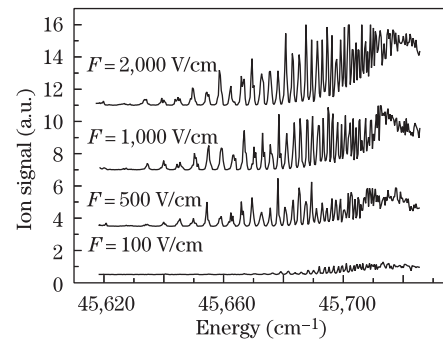


Fig. 3. EFI spectra of Eu atoms obtained at different electric field strengths.

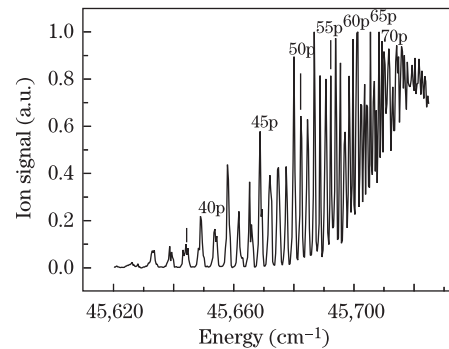


Fig. 4. EFI spectrum of the Eu atomic $4f^7 6s(^9S)np$ Rydberg series at $F = 2 \text{ kV/cm}$.

a pulsed electric field has to be maintained at a higher strength.

As shown in Fig. 2(a), only a few peaks can be detected below the ionization limit, while many higher members of the Rydberg series appear in Fig. 2(b). This obvious difference confirms that detection with the EFI method is much more efficient than that with photoionization. On the other hand, in both Figs. 2(a) and (b), there is a narrow peak A and a wide profile B, which is above or across the first ionization limit $4f^7 6s(^9S)_4$. Obviously, both have a much larger width than those of bound states due to the interaction with the related $4f^7 6s(^9S)\epsilon p$ continuum states. Peak A can be identified as one of the $4f^7 5d 7p(^8P_J)$ autoionizing states.

Based on the additional effort from this work and comparisons with a previous one^[9], we may assign the J value of peak A as $7/2$ or $9/2$. On the other hand, the B profile has not been observed previously, but it exists in both detection cases. A possible assignment to this profile is the $4f^7 5d 7p(^8P_J)$ state. The large width indicates its profound configuration interaction with the $4f^7 6s(^9S)\epsilon p$ continuum states. Similar phenomena have been observed in the cases of the Ba and Yb atoms, where the $5dnp$ states interact strongly with the $4f^7 6s(^9S)\epsilon p$ states near the $6s^+$ ionization limit.

To determine the close relationship between EFI spectra with the strength of an applied electric field, it is helpful to measure the spectra with different strengths of electric field, an example of which is shown in Fig. 3.

The weakly bound Rydberg atom is highly sensitive to the external electric field because the Rydberg electron moves in a larger orbit. As shown in Fig. 3, lower- n members of the Rydberg series can be detected when the electric field strength is increased. For example, the

Table 1. Spectral Information on the Eu $4f^76s(^9S)np^8P_J$ Rydberg States with $J=5/2, 7/2, \text{ or } 9/2$. The Rydberg Series of the Eu Atom is Converging to the First Ionization Limit $4f^76s^9S_4$

N	E (cm $^{-1}$)	n^*	δ	E (cm $^{-1}$) ^[9]
40	45650.28	36.01	3.99	
41	45654.70	36.99	4.01	
42	45658.82	37.98	4.02	45658.74
43	45662.65	38.97	4.03	45662.57
44	45666.15	39.95	4.05	45666.13
45	45669.54	40.98	4.02	45669.43
46	45672.33	41.88	4.12	45672.53
47	45675.25	42.89	4.11	45675.37
48	45677.84	43.85	4.15	45678.00
49	45680.40	44.87	4.13	45680.53
50	45682.73	45.86	4.14	45682.86
51	45684.90	46.85	4.15	45685.03
52	45686.88	47.80	4.20	45687.12
53	45689.00	48.90	4.10	45689.05
54	45690.62	49.78	4.22	45690.82
55	45692.51	50.88	4.12	45692.50
56	45694.13	51.88	4.12	45694.05
57	45695.54	52.80	4.20	45695.50
58	45697.01	53.82	4.18	45696.87
59	45698.32	54.77	4.23	45698.16
60	45699.71	55.84	4.16	45699.40
61	45700.78	56.71	4.29	45700.57
62	45701.86	57.63	4.37	45701.70
63	45703.19	58.83	4.17	
64	45704.00	59.59	4.41	
65	45705.18	60.76	4.24	
66	45705.97	61.59	4.41	
67	45707.07	62.79	4.21	
68	45707.86	63.70	4.30	
69	45708.70	64.72	4.28	
70	45709.51	65.74	4.26	
71	45710.30	66.79	4.21	
72	45710.85	67.55	4.45	

ionization signals of lower- n states are increased more through several orders of magnitude at $F=2$ kV/cm compared to those at $F=100$ V/cm. To view details of the higher- n members of the Eu $4f^76s(^9S)np^8P_J$ ($J=5/2, 7/2, 9/2$) Rydberg series, an observed EFI spectrum at $F=2$ kV/cm is shown in Fig. 4.

As shown in Fig. 4, the Eu atom is excited to the $4f^76s(^9S)np$ Rydberg series from the $4f^76s7s^8S_{7/2}^o$ state in the energy region from 45,620 to 45,725 cm $^{-1}$, just below the ionization limit $4f^76s^9S_4$ at 45,734.92 cm $^{-1}$ ^[5]. Due to the fine structures, there are several Rydberg series converging to this ionization limit. Unlike the situation in the lower energy region where the fine structures can be resolved, the spectral feature near the ionization limit actually represents a convolution of several fine structure transitions.

To determine the energy values E of any peak in Fig. 4, one should determine its λ_3 value first and then use the relation $E=1/\lambda_1+1/\lambda_2+1/\lambda_3$ to obtain its level energy in wave number (cm $^{-1}$). Due to limitations from the laser line width used in the experiment, only energies of the $4f^76s(^9S)np$ states below 45,710 cm $^{-1}$ can be determined. Typical experimental uncertainties of the energy

values are better than ± 0.1 cm $^{-1}$.

Compared with the previous experiment^[9] on the Eu $4f^76s(^9S)np$ Rydberg series carried out with absorption spectroscopy, the present work not only uses a different method, but also covers a greater energy range. Under an electric field with a strength less than 2 kV/cm, the Eu atom in the $4f^76s(^9S)np^8P_J$ states can be detected, where $40 \leq n \leq 72$. Thus, this work not only confirms the reported level energies for the $n=42\sim 62$ states (Table 1), but also determines more $4f^76s(^9S)np$ Rydberg states. The n -assignment is based on known n values from the lower members^[9]. Once the n and n^* values for a Rydberg state are known, the quantum defect δ for this state can be determined by $\delta = n - n^*$.

The level energies of many states with their n -assignment information are listed in Table 1, including the n -value, effective quantum number n^* , and quantum defect δ . From Table 1, δ clearly increases linearly with n , which is no longer a constant. The possible reason for this departure is the perturbation from the other Rydberg series.

In conclusion, the EFI method is successfully used to detect the Eu $4f^76s(^9S)np^8P_J$ Rydberg states with $40 \leq n \leq 72$. Due to limitations of the laser line width, the states as high as $n=72$ of this series can be resolved. This work not only confirms previous data on the level energy of the $4f^76s(^9S)np^8P_J$ states, but also significantly extends the n -value to the higher direction. The data obtained in this work will enrich knowledge on the Eu atom and stimulate further theoretical efforts to improve the quantum theory for complex atomic systems.

This work was supported by the National Natural Science Foundation of China (No. 10674102) and the Natural Science Foundation of Tianjin (No. 05YFJMJC05200).

References

1. C. J. Dai, Phys. Rev. A **52**, 4416 (1995).
2. C. J. Dai, Phys. Rev. A **51**, 2951 (1995).
3. J. Lu, C. Dai, C. Lee, Y. Xu, Z. Liu, and J. Tang, Acta Opt. Sin. (in Chinese) **20**, 908 (2000).
4. J. Xie, C. Dai, and M. Li, Acta Opt. Sin. (in Chinese) **30**, 2142 (2010).
5. S. G. Nakhate, M. A. N. Razvi, J. P. Connerade, and S. A. Ahmad, J. Phys. B At. Mol. Opt. Phys. **33**, 5191 (2000).
6. S. Bhattacharyya, R. D'souza, P. M. Rao, and M. A. N. Razvi, Spectrochimica Acta Part B **58**, 469 (2003).
7. S. Bhattacharyya, M. A. N. Razvi, S. Cohen, and S. G. Nakhate, Phys. Rev. A **76**, 012502 (2007).
8. Y. Xiao, C.-J. Dai, and W.-J. Qin, Chin. Phys. B **18**, 4251 (2009).
9. G. Smith and F. S. Tomkins, Proc. R. Soc. Lond. A **342**, 149 (1975).
10. M. D. Lindsay, C. J. Dai, B. J. Lyons, C. R. Mahon, and T. F. Gallagher, Phys. Rev. A **50**, 5058 (1994).
11. S. Li and C. Dai, J. Electron Spectrosc. Relat. Phenom. **136**, 247 (2004).
12. C. J. Dai, S. Zhang, X. W. Shu, D. W. Fang, and J. Li, J. Quant. Spectro. Radia. Trans. **53**, 179 (1995).